

Gravitational-wave radiation from double compact objects with eLISA in the Galaxy.

Jinzhong Liu¹ and Yu Zhang¹

ABSTRACT

The phase of in-spiral of double compact objects (DCOs: NS+WD, NS+NS, BH+NS, and BH+BH binaries) in the disk field population of the Galaxy provides a potential source in the frequency range from 10^{-4} to 0.1 Hz, which can be detected by the European New Gravitational Observatory (NGO: eLISA is derived from the previous LISA proposal) project. In this frequency range, much stronger gravitational wave (GW) radiation can be obtained from DCO sources because they possess more mass than other compact binaries (e.g., close double white dwarfs). In this study, we aim to calculate the gravitational wave signals from the resolvable DCO sources in the Galaxy using a binary population synthesis approach, and to carry out physical properties of these binaries using Monte Carlo simulations. Combining the sensitivity curve of the eLISA detector and a confusion-limited noise floor of close double white dwarfs, we find that only a handful of DCO sources can be detected by the eLISA detector. The detectable number of DCO sources reaches 160, in the context of low-frequency eLISA observations we find that the number of NS+WD, NS+NS, BH+NS, and BH+BH are 132, 16, 3, and 6, respectively.

Subject headings: binaries: general — stars: evolution — gravitational waves

1. Introduction

Gravitational waves (GWs) are a natural result of Einstein's theory of gravity resulting from a space perturbation of the metric traveling at the speed of light. This phenomenon of space-time has still not been directly observed on the ground such as LIGO or VIRGO, because there exist seismic and gravity gradient noise. The observation of the binary pulsar PSR 1913+16, which is a neutron star plus neutron star (NS+NS) system, has given an indirect evidence of GW radiation (Hulse & Taylor 1975; Taylor & Weisberg 1982). Therefore, the European New Gravitational Wave Observatory (NGO is referred to as eLISA) mission will search the GW radiation in the frequency band between 10^{-4} Hz and 0.1 Hz, which is the previous LISA's heritage (Amaro-Seoane et al 2012, and references

therein). The main GW sources in this frequency range are extreme mass ratio inspirals (EMRIs) of stellar-mass compact objects orbiting the massive black holes (BHs) (e.g., Glampedakis 2005; Hopman & Alexander 2006), the coalescence of super-massive BH binaries of merging galaxies (e.g., Iwasawa et al. 2011; Liu et al. 2012) and Galactic compact double binaries (e.g., Hils et al. 1990; Ruiter et al. 2010). For example, due to the largest population in the Galaxy, close double white dwarfs (DWDs) are believed to dominate the Galactic GW foreground radiation that generate a confusion-limited noise floor for the classical LISA detector, with several thousand of the higher GW radiation signal sources being possibly resolved (e.g., Evans et al. 1987; Hils et al. 1990; Nelemans et al. 2001; Liu 2009; Liu et al. 2010a,b; Littenberg 2011; Nissanke et al. 2012; Shah et al. 2012, 2013; Nelemans 2013). In this study, we focus on other types of double compact binaries (DCOs): neutron star plus white dwarf (NS+WD), double neutron star binaries

¹National Astronomical Observatories/Xinjiang Observatory, Chinese Academy of Sciences, 150 Science 1-street Urumqi, 830011 Xinjiang, P. R. China. liujinzh@xao.ac.cn

(NS+NS), black hole plus neutron star (BH+NS), and double black hole (BH+BH) binaries. Few studies investigate the importance of these GW sources because these objects are much rarer than the DWD binaries. However, DCOs can radiate stronger GW signals because of higher mass than WDs.

As a physical reality event, DCOs play an important role in stellar evolution of population synthesis studies (Tutukov & Yungelson 1994; Dewi & Pols 2003; Wang et al. 2009; Chen et al. 2011; Zhang et al. 2012; Jiang et al. 2012), because they are expected to be potential progenitors of related objects, such as ultra-compact X-ray binaries (e.g., van der Sluys et al. 2005) and short-hard γ -ray bursts (e.g., Eichler et al. 1989; Paczynski 1991; Narayan et al. 1992). Meanwhile, the final merger processes of the DCOs are expected to be a type of high frequency GW sources for the ground-based GW detectors (such as LIGO or VIRGO). In this class of compact binaries, their merger rates and birth rates are still an open question, especially for systems containing BHs (Abadie et al. 2010b). Several double NSs (NS+NS) are currently detected through searching binary pulsars, only PRS J0703–3039 (Burgay et al. 2003) belongs to the eLISA frequency ranges, and BH or BH+NS systems have not been observed so far. Therefore a binary population synthesis (BPS) approach has been applied to evaluate the merger rates of DCOs (Hurley et al. 2000, 2002; Han et al. 2007), and this method has also been systematically used to study the GW radiation in the Galaxy (Nelemans et al. 2001; Liu 2009).

In this study, we analyze the DCO systems as GW sources in the disk field population that obtained from a BPS model, and address the GW radiation from these sources comparing with the sensitivity curve of the eLISA detector and the confusion-limited noise floor of DWD systems. This study can be used to determine the binary parameters when the BH/NS in-spiral processes can be detected by GW detectors in future. In the next section, the model is described. In Sect. 3, we present the results and discussion in our simulations.

2. Model

The stellar evolution was based on the work previously presented by Hurley et al. (2000) and Hurley et al. (2002). The method of calculating GW radiation from double white dwarf systems, combined with the noise curve of LISA, was described by Liu (2009) and Liu et al. (2010a). Here we use this BPS method (Liu 2009; Liu et al. 2010a) in the same way to investigate the importance of GW radiation from DCO systems with the eLISA in the Galaxy. Below we briefly summarise this method in the current study.

In the BPS model, the rapid binary stellar evolution (BSE) code (Hurley et al. 2000, 2002) was used to investigate the evolution of binary stars. This BSE code was built on the Cambridge stellar evolution tracks (Eggleton 1971, 1972, 1973), and the input physics were updated by Han et al. (1994) and Pols et al. (1995), and various initial distributions of components are performed using a Monte Carlo simulation including the initial mass function (IMF) of primary, the initial mass ratio, the initial orbital separation, the initial eccentricity and the binary space model in the Galaxy. This code provides an opportunity for calculating the evolution of a binary by given its zero-age main-sequence mass (ZAMS) and metallicity. For these DCO sources, we need to obtain the evolutionary results at the formation of a stellar remnant: a WD, a NS, or a BH. Some of the most relevant features (e.g. wind accretion, orbital changes due to mass variations, tidal evolution, magnetic braking, supernovae kicks, roche lobe overflow, common-envelope evolution, coalescence of common-envelope cores, and collision outcomes) of the BSE code can be found in Hurley et al. (2002).

For the component WD of NS+WD system, three types of WDs are distinguished in the BSE simulation: a He WD (formed by complete envelope loss of a first giant branch star with mass less than the maximum initial mass of igniting in a helium flash), a CO WD (formed by envelope loss of a thermally pulsing asymptotic giant branch star), and Oxygen/Neon WD (envelope loss of a thermally pulsing asymptotic giant branch star). Note that if the CO WD accretes enough mass M_{acc} , then this CO WD will explode without leaving a remnant, while an Oxygen/Neon WD

leaves a NS depending on the hypotheses on the use of accretion-induced collapse (AIC) (Nomoto & Kondo 1991). In the BSE code, the value of Chandrasekhar is always given by $M_{\text{Ch}} = 1.44M_{\odot}$.

If a NS or BH is obtained from the BPS simulation, its gravitational mass can be evaluated by

$$M_{\text{NS}} = 1.17 + 0.09M_{\text{c,SN}}, \quad (1)$$

where $M_{\text{c,SN}}$ is the mass of the CO-core when the supernova explosion is occurred.

During an asymmetry explosion process, a velocity kick can be produced from an explosion with leaving a remnant (a NS or a BH) (Lyne & Lorimer 1994). To obtain the kick velocity \mathbf{v}_k , we choose the kick speed from a Maxwellian distribution

$$P(v_k) = \sqrt{\frac{2}{\pi}} \frac{v_k^2}{\sigma_k^3} e^{-v_k^2/2\sigma_k^2}. \quad (2)$$

We use velocity dispersion $\sigma_k = 190\text{km/s}$, which is consistent with the data on pulsar proper motions (Hansen & Phinney 1997). Note that we only refer to the DCO objects in the Galaxy field population using a thin disk model (Equ. 13 of Liu 2009), and exclude the DCOs resided in halo and bulge from our simulation. That is because that most of these DCO binaries have long orbital periods ($P_{\text{orb}} > 5.6$ hrs corresponding to $\log f < -4.0$ Hz) leading to relative small contributions to GW signals (Belczynski et al. 2010). And the dynamical interacting (e.g., evolution of stars in the globular clusters) in the Galaxy is not considered in the current study. We note that the binary stellar evolutionary channels lead to the production of DCOs with circular orbits, even if the ZAMS eccentricity is non-zero in the simulation, because tidal circularization and synchronization are rapid when a system contains a near-Roche lobe-filling convective star. This is an assumption in the BSE code.

Table 1 Parameters for three types of compact remnant objects obtained from the binary evolution.

Initial mass [M_{\odot}]	remnant object	mean remnant mass [M_{\odot}]
$0.32 < M < 8$ –12	WD	0.58
8 –12 < $M < 25$ –45	NS	1.39
25 –45 < $M < 100$	BH	9.5

By means of a BSE code and a Monte Carlo simulation, we get three types of remnant objects,

that is, WD, NS, and BH. Meanwhile, the initial basic parameters and descriptions are as follows in the BSE code: the tidal enhancement of the stellar wind B is 1000, the mass transfer efficiency for stable Roche lobe overflow (RLOF) is 0.5, the ejection efficiency parameter of a common envelope (CE) is 1, the stellar wind velocity is 20km/s, and the solar metallicity Z is 0.02. And we also assume a constant star formation rate (SFR) over the last 13.7Gyr in the simulation. The detailed descriptions of these parameters can be found in some studies (Han 1998; Hurley et al. 2002). Therefore, we can trace the evolution of these objects using the BSE code and calculate the boundaries for the initial masses of progenitors of WDs, NSs and BHs. The mass parameters for these three types of DCO objects are summarized in Table 1. Indeed, these acceptable values of initial mass and mean remnant mass listed in Table 1 are in common with other studies (Han 1998; Ziolkowski 2010). In addition, Belczynski et al. (2010) have investigated the importance of supernova kicks in BH or NS formation processes. We assume $\sigma_k = 190\text{km/s}$ as a input parameter in the BSE code.

In this study, a two year mission lifetime is assumed, a width of a resolvable frequency bin is $\Delta f = 1/T_{\text{obs}} = 1.6 \times 10^{-8}$ Hz. Petiteau et al. (2008) showed the eLISA/NGO sensitivity curve, which averaged over all sky locations and polarizations and did not include the foreground noise of close white dwarfs. And based on this sensitivity curve, we create the time series for the source signals and add the individual time series of the calculated sources to produce the total data stream. Similar calculations of the GW signal analysis combined with a GW detector can be found in Timpano et al. (2006), Liu (2009) and Nissanke et al. (2012). Note that we should select all DCO systems that have a signal above the (signal-to-noise ratio: $S/N = 7$) sensitivity limit of the eLISA detector. In this study, $S/N > 7$ is considered the lowest acceptable threshold.

3. Results and discussion

Basing on a population synthesis code, from a sample of 10^7 binaries, we obtain DCO (NS+WD, NS+NS, BH+NS, and BH+BH) systems. According to the evolutionary trace of these four types of DCOs in the BSE code, we give the descriptions of

physical properties (e.g., birth rates, distributions of orbital frequency, and chirp mass) and the GW radiation contributions of these DCO sources.

On the basis of evidence in section 2, in table 2 we list the Galactic birth rates and total numbers for four types of DCOs from the BPS simulation and the number of systems that can be detected by the eLISA detector. From this, we see that the detectable number of all DCO sources is 157. The NS+WD detectable sources reach 84.1% of the total DCOs, the percentages are 10.2% for NS+NS systems, and 5.70% for BH+NS and BH+BH binaries. Within the entire DCO binaries predicted for the present time in our Galaxy disk, NS+WD sources are supreme (73.7%), with a chief contribution of NS+NS (25.8%) systems, and a very small fractions of BH+NS and BH+BH (0.500%) sources. We note that investigating the different input parameters from BPS simulation can change the maximum percentage uncertainty of DCO systems up to a factor of ~ 3.25 . This shows that the number of DCO systems is consistent with the Galactic birth rate in table 2. Note that the number quoted here is based on the assumption that one binary with $M_1 > 0.8M_\odot$ is formed per year in our Galaxy (Iben & Tutukov 1984; Yungelson et al. 1993), and one assumes a constant star formation rate $\text{SFR} = 5M_\odot/\text{yr}$, where $5M_\odot$ stands for the average binary mass. In table 2 the DCO systems' birthrate in the Galaxy is the convolution of the distribution of the delay times (DDT) with the star formation rate (SFR) (Greggio et al. 2008). Due to a constant SFR, the birthrate of DCO systems is only related to the DDT, which reveals a function relation in different formation times of DCOs. Finally, in our simulation we also assume a solar metallicity $Z = 0.02$ and 100% binaries. Additionally, the DCO systems with mass-transfer or merged are excluded from the BPS simulation.

Table 2 Galactic birth rates and total numbers for four types of DCOs from the BPS simulation and the number of systems than can be detected by the eLISA detector.

Type	Total DCOs	Birth Rate (10^{-5}yr^{-1})	Detectable sources above noise
[NS, WD]	191343	53	132
[NS, NS]	66816	2.8	16
[BH, NS]	367	1.3×10^{-2}	3
[BH, BH]	876	0.17	6

3.1. The orbital frequency distribution of DCO systems

The orbital frequency of a DCO will increase due to GW radiation, so the orbital frequency is an important physical characteristic in the present study. In Figure 1, we present the distribution of orbital frequency for four types of DCOs including NS+WD, NS+NS, BH+NS, and BH+BH. From this, we see that the orbital frequency distributions are different for four types of DCO systems, which are characterized by one or two distinct peaks. For NS+WD systems, a notably higher narrow peak occurs at $\log f = -3.35\text{Hz}$ ($P_{\text{orb}} \sim 1.24\text{hrs}$) and nearly 50% of numbers are less than a vale of orbital frequency $\log f = -4\text{Hz}$ with a shorter broad peak at $\log f = -4.6\text{Hz}$ ($P_{\text{orb}} \sim 22.1\text{hrs}$). For NS+NS systems, most of samples are gathered in the orbital frequency range 10^{-4} to 10^{-5}Hz ($P_{\text{orb}} \sim 5.6 - 55.6\text{hrs}$). For BH+NS systems, a high peak is appeared in the orbital frequency $\log f = -4.2\text{Hz}$ ($P_{\text{orb}} \sim 8.8\text{hrs}$). For BH+BH systems, we note that the orbital frequency distribution is similar to the case of BH+NS, the differences are not very large besides the peak value $\log f = -4.7\text{Hz}$ ($P_{\text{orb}} \sim 27.8\text{hrs}$).

We can know two kinds of information from Figure 1. Firstly, Podsiadlowski et al. (2003) shown that the formation of a NS or a BH in a binary system should experience a CE event, and this time-scale in formation of CE process is often dynamically unstable (Paczynski 1976). If double NS (or BH) binaries that enter the RLOF as events, they always coalesce immediately as possible γ -ray bursts. In this present work, we assume that if there is not enough orbital energy to release the CE, it leads to a merger when a common envelope is formed. We note that the formation channel for a maximum value in each panel of Figure 1 is shaped by the CE phase. Specially, at orbital frequencies above 10^{-3}Hz (corresponding to a shorter orbital period less than 0.56 h), the DCO systems are obtained from two successive CE evolutionary phase, and they are resolved sources (See section 3.3). This is because that dynamically unstable mass transfer is expected to lead to the formation of a CE. And because of more CE evolution phases, the evolution of more massive progenitors trend to produce DCO binaries with shorter orbital periods (Han 1998). Secondly, a synchronization time-scale (Hurley et al. 2002)

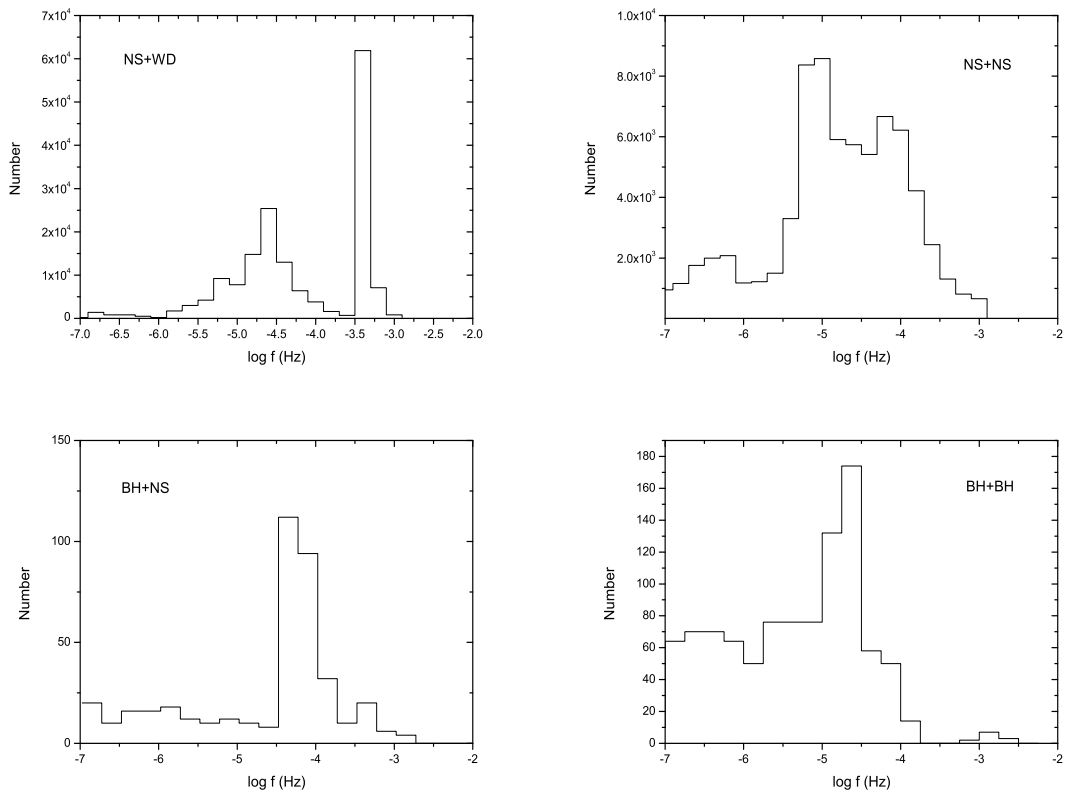


Fig. 1.— Distribution of orbital frequency for four types of DCOs at the present time in the Galaxy including NS+WD, NS+NS, BH+NS, and BH+BH.

can affect the formation of DCO binaries, because the components may be spun up by mass transfer. For example, a WD-NS binary with a separation 10 times the WD radius would have a very long circularization time-scale ($\sim 10^{14}\text{yr}$), thus the degenerate damping is dominant only for WD-NS systems in which the separation can become very small. For the extreme conditions of short orbital period sources (e.g, AM CVn stars and ultra-compact X-ray binaries) in the BPS simulations, we note that the information on the physics of tides and the stability of the mass-transfer processes is not investigated in the current study.

3.2. The chirp mass distribution of DCO systems

A binary system radiates GWs and loses angular momentum, so the separation decreases and the GW amplitude increases, which leads to a measurable characteristic “chirp” signal. According to the definition of “chirp mass” for a binary system $\mathcal{M}_{\text{chirp}} = m_1^{3/5} m_2^{3/5} (m_1 + m_2)^{-1/5}$, Schutz (1996) displayed the frequency evolution of a binary due to GW radiation. In practice, for high-frequency binaries, this means that during a long observation time T_{obs} , the “chirp” signal can be detected by the eLISA detector (Evans et al. 1987).

In Figure 2, we present the chirp mass distribution for four types of DCOs in our model. From this we find that the averages of the chirp mass for the NS+WD, NS+NS, BH+NS, and BH+BH are $0.93M_{\odot}$, $1.27M_{\odot}$, $2.50M_{\odot}$, and $7.13M_{\odot}$, respectively. Note that the chirp mass of PSR J0737-3039 (NS+NS) is $1.13M_{\odot}$ (Lyne et al. 2004), which is not much different from our calculations within a deviation $\sigma_{\mathcal{M}_{\text{chirp}}} = 0.14M_{\odot}$. We also find that the chirp mass distributions are very different for the four subclasses. For NS+WD systems, they bridge a narrow range: $\mathcal{M}_{\text{chirp}} \sim 0.72 - 1.27M_{\odot}$ and peak at $\mathcal{M}_{\text{chirp}} \sim 0.95M_{\odot}$. For NS+NS systems, a well-known narrow peak occurs at $\mathcal{M}_{\text{chirp}} \sim 1.17M_{\odot}$ with a stepping tail that extends to $\mathcal{M}_{\text{chirp}} \sim 1.57M_{\odot}$. For BH+NS and BH+BH systems, the chirp mass distributions have a wide range: $\mathcal{M}_{\text{chirp}} \sim 1.8 - 3.2M_{\odot}$ for BH+NS and $\mathcal{M}_{\text{chirp}} \sim 5.7 - 10.8M_{\odot}$. A resolved chirping DCO binary can be used to measure the luminosity distance to the source directly, based on the chirp line for $T_{\text{obs}} = 2\text{yrs}$ (e.g., Equ.6 of

Nelemans 2001) we find that the number of resolvable DCO binaries with the chirping signal is 136.

As displayed above, the significantly different results can be explained as follows. Firstly, a comparative distribution of NS+NS and BH+BH binaries with a similar shape depends not only on the choice of single star mass when BHs (or NS) are formed, but also, at some level, on the assumption that an NS collapses to a BH when it accretes enough material to its mass above $1.8M_{\odot}$ (Bombaci 1996). This mass is not well constrained. In this work, if an ONeWD or COWD accretes CO or ONe material, which swelled up around these compact cores, and this new mass exceeds the Chandrasekhar mass, M_{Ch} , so the process of electron capture on ^{24}Mg nuclei leads to an AIC process (Nomoto & Kondo 1991) and the formation of an NS. Meanwhile, whether a condition of thermonuclear explosion is actually not clear. The temperature produced at the core–disk boundary mostly depends on the accretion rate. If the temperature is hot enough to ignite carbon and oxygen, then the WD is converted to an ONeWD relies on competition between the rate of propagation of the flame inwards, which is judged by the opacity, and the cooling rate of the WD. All of the uncertainty can influence the mass determination of NS (or BH), and then affect the GW radiation characteristic parameter $\mathcal{M}_{\text{chirp}}$. Secondly, for BH+BH (or BH+NS) systems it is obvious that the BH mass is the decisive factor leading to the calculation of chirp mass. Note that the chirp mass coverage range ($\mathcal{M}_{\text{chirp}} \sim 1.8 - 10.5M_{\odot}$) predicted in the disk population of Galaxy is consistent with the results of stellar mass population of Galactic BHs with high metallicity environment (Ziolkowski 2010). Thirdly, the phase of dynamical mass transfer plays an important role in the formation BH or NS. For example, dynamical mass transfer of helium or CO on to a COWD or ONeWD causes the formation of a thick accretion disk around the more massive WD ($M + \Delta M$), and the coalescence is happened over a viscous time-scale. If the mass of $M + \Delta M > M_{\text{Ch}}$, it explodes as a possible type Ia SN (Branch 1998), leaving no remnant. But a spherically symmetric evolution model of Saio & Nomoto (1998) suggested that the AIC NS can be also formed rather than type Ia SNe although the mass greater than M_{Ch} .

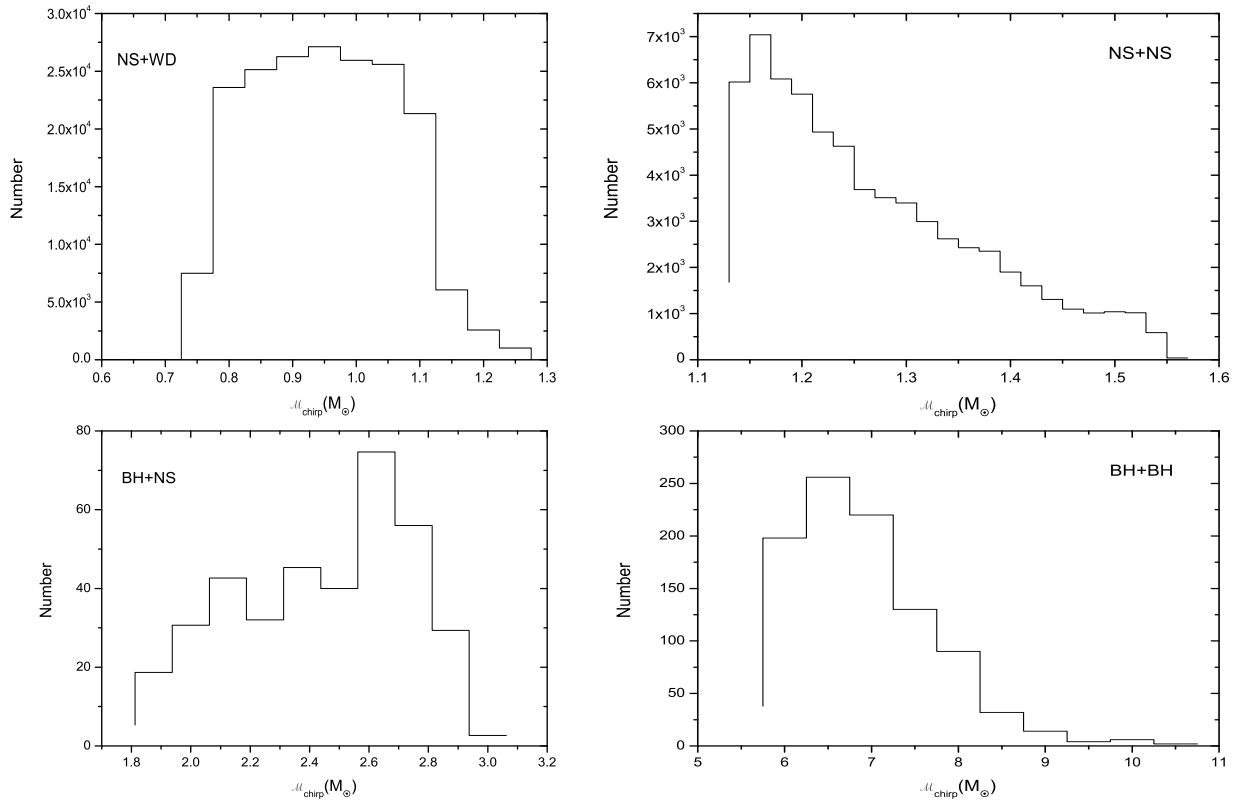


Fig. 2.— The same as Figure 1 but for the distribution of chirp masses for the DCO systems.

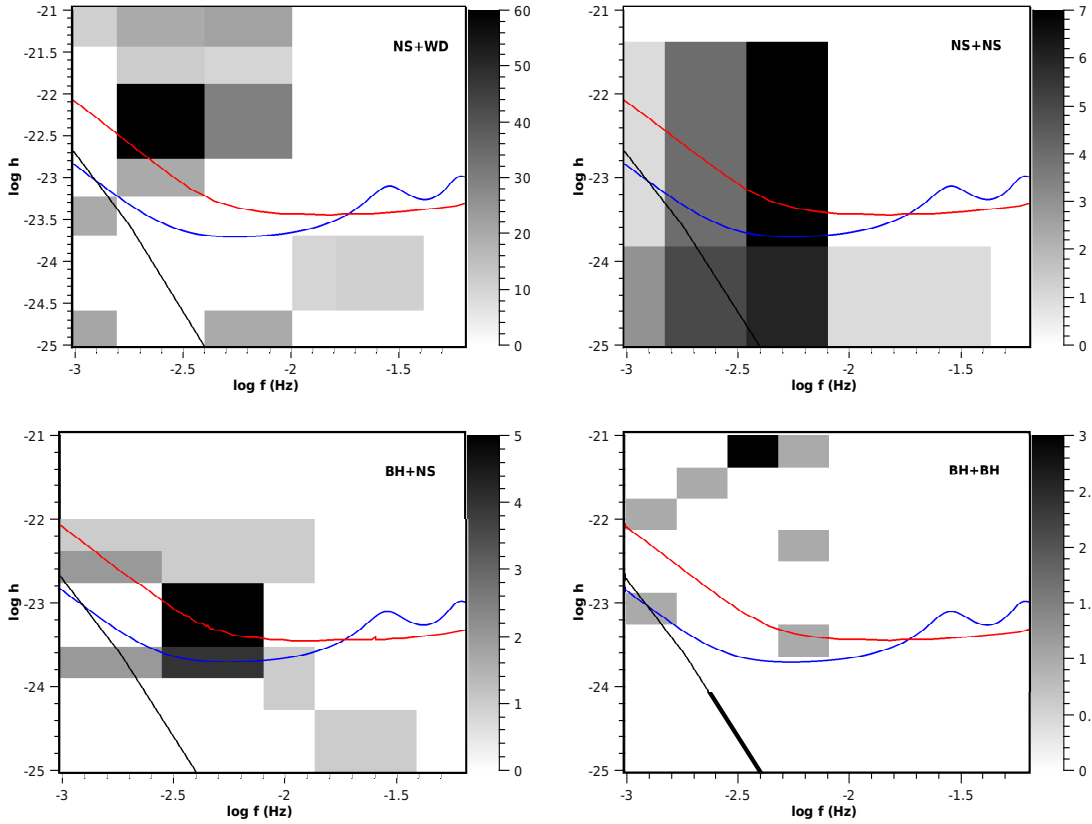


Fig. 3.— Similar to Figure 1, but for the strain amplitude h as a function of the frequency for four types of DCO systems. In each panel, the grey shade displays the density distribution of the resolved systems; the black line gives the averaged GW foreground due to a contribution of DWD systems in the Galaxy (Liu 2009); the red line stands for the expected eLISA sensitivity curve using the simulator LISA-Code 2.0 (Petiteau et al. 2008). For a reference, we also display the sensitivity curve (blue line) of previous LISA detector (Larson et al. 2000).

Meanwhile the Eddington limit (Cameron 1967) is considered in the accreted material of WD, NS or BH.

3.3. The GW radiation signature for resolved sources

According to the description of criterion in previous studies (Liu 2009; Liu et al. 2010a), which can be summarized as “one bin rule + the average foreground noise of DWDs + the eLISA sensitivity curve”, the detectable numbers for four types of DCOs from the BPS simulation have been listed in Table 2. In Figure 3, we separate out the different kinds of DCOs in each panel. We plot the GW radiation distribution from the resolved sources (the grey shades) for four types of DCO systems. We also display the sensitivity limits of previous LISA (Larson et al. 2000). The solid line stands for the average foreground that are produced by DWDs (Liu 2009). From this, in each panel we can see that only a few DCOs can be detected by the eLISA detector, which has become less sensitive than previous LISA.

The main purpose of this study is to find out how many resolved DCO sources we can explore with an instrument like the eLISA detector from the GW radiation. For “one bin rule”, we assume that at least one frequency in the eLISA data can be detected as GW sources. Here we refer to “one bin rule”, we aim to see whether the individual DCO sources can be detected by the eLISA detector with one resolvable bin ($\Delta f = 1.6 \times 10^{-8} \text{Hz}$). The DCO binaries, which are the only ones in their corresponding resolvable bins and their strains are higher than the noise curve (including the sensitivity curve of eLISA detector and the foreground noise of DWDs), are called detectable sources. A detected source with frequency f and strain amplitude h that is observed over a time T_{obs} will appear in the Fourier spectrum of the data as a single spectral line. We note that this method is applicable to the Galactic population of detached binaries (e.g., DWDs and DCOs), and is discussed by the characterization GW signal in a mass-transferring system (Timpano et al. 2006). For “the average foreground noise of DWDs”, we use an exponential decay shape to modify the average foreground noise from detached DWDs in the Galaxy (Liu 2009), which is not a Gaussian shape and does not include the loudest resolved WD pop-

ulations. For “the eLISA sensitivity curve”, comparing the GW strain amplitude from a DCO system with the average foreground noise of DWDs we can see that whether the individual sources can be detected by the eLISA detector.

Undoubtedly, comparing with previous studies we find that there exist individual resolved DCO systems in the disk of the Galaxy above the predicted average foreground noise of DWDs and the eLISA sensitivity curve, which is likely to be used in the GW study. The estimation of GW radiation agrees well with Nelemans et al. (2001) and Belczynski et al. (2010), although these authors used different binary evolution assumptions in the BPS model for the underlying DCO population. For example, the change of the binary orbital periods in this work is governed by conservation of angular momentum rather than energy, and during a CE evolution phase a DCO system can have a shorter orbital period using the α formalism than ones using γ formalism. Therefore, for the detectable number of DCO sources (e.g., NS+NS, BH+NS, BH+BH), Nelemans et al. (2001) cited those number as 38–124, 8–31 and 0–3, while Belczynski et al. (2010) displayed 0.4–5, 0–0.6 and 0–3.5 respectively. Due to so many assumptions as input as BPS simulations, we need to note that there exists uncertainties in this prediction. We have studied the effect of different physical parameters (e.g., the ejection parameter of CE, the mass transfer or stellar wind parameter, and tidal evolution) and the various initial distributions of components (e.g., e , IMF and q) on the GW radiation from DCOs. We find that the number of detectable sources of NS+WD, NS+NS, BH+NS, and BH+BH can range from 62 to 429, 7 to 52, 0 to 10, and 0 to 19, respectively. Additionally, a form of understanding the CE evolution mechanism is provided by the DCO binaries whose characteristics can be investigated if a significant amount of angular momentum and mass have been removed from the precursor system. Finally, we have not included any GW signals from EMRIs and super-massive black hole in-spirals in this work.

To summarize, we create a population of DCO systems using a Monte Carlo simulation and discuss the importance of some physical process and parameters on the formation of DCO systems in detail. Although the presence of many uncertain

factors (e.g., the CE evolution question) should influence the outcome of this work, a simulation of the GW radiation from DCO systems has been still carried out using the BPS model. We present the distributions of orbital frequencies and chirp masses for DCO systems that are observable with the eLISA detector in a one-year observation. The total resolvable numbers of DCOs can take up to 200, and we find that the estimate for the number of resolved DCO sources ranges from 5 to 167.

We thank Prof. Han Zhanwen at Yunnan Observatory for valuable comments. This work is supported by the program of the Xinjiang Natural Science Foundation (No. 2011211A104), Natural Science Foundation (No. 11103054 and 11303080) and light in China's Western Region (LCWR) (No. XBBS201022 and XBBS201221). This project/publication was made possible through the support of a grant from the John Templeton Foundation. The opinions expressed in this publication are those of the authors and do not necessarily reflect the view of the John Templeton Foundation. The funds from John Templeton Foundation were awarded in a grant to The University of Chicago which also managed the program in conjunction with National Astronomical Observatories, Chinese Academy of Sciences (No. 100020101)

REFERENCES

- Abadie, J., et al. 2010a, *ApJ*, 715, 1453
- . 2010b, *Classical and Quantum Gravity*, 27, 173001
- Amaro-Seoane, P., et al. 2012, *Classical and Quantum Gravity*, 29, 124016
- Belczynski, K., Benacquista, M., & Bulik, T. 2010, *ApJ*, 725, 816
- Benacquista, M. J., Larson, S. L., & Taylor, B. E. 2007, *Classical and Quantum Gravity*, 24, 513
- Bombaci, I. 1996, *A&A*, 305, 871
- Branch, D. 1998, *ARA&A*, 36, 17
- Burgay, M., et al. 2003, *Nature*, 426, 531
- Cameron, A. G. W. 1967, *Nature*, 215, 464
- Carr, B. J., & Hawking, S. W. 1974, *MNRAS*, 168, 399
- Chen, X., Han, Z., & Tout, C. A. 2011, *ApJ*, 736, L40
- Dewi, J. D. M., & Pols, O. R. 2003, *MNRAS*, 344, 629
- Eggleton, P. P. 1971, *MNRAS*, 151, 351
- . 1972, *MNRAS*, 156, 361
- . 1973, *MNRAS*, 163, 279
- Eggleton, P. P., Fitchett, M. J., & Tout, C. A. 1989, *ApJ*, 347, 998
- Eichler, D., Livio, M., Piran, T., & Schramm, D. N. 1989, *Nature*, 340, 126
- Evans, C. R., Iben, Jr., I., & Smarr, L. 1987, *ApJ*, 323, 129
- Fryer, C., & Kalogera, V. 1997, *ApJ*, 489, 244
- Glampedakis, K. 2005, *Classical and Quantum Gravity*, 22, 605
- Goldberg, D., & Mazeh, T. 1994, *A&A*, 282, 801
- Greggio, L., Renzini, A., & Daddi, E. 2008, *MNRAS*, 388, 829
- Han, Z. 1998, *MNRAS*, 296, 1019
- Han, Z., Eggleton, P. P., Podsiadlowski, P., & Tout, C. A. 1995, *MNRAS*, 277, 1443
- Han, Z., Podsiadlowski, P., & Eggleton, P. P. 1994, *MNRAS*, 270, 121
- Han, Z., Podsiadlowski, P., & Lynas-Gray, A. E. 2007, *MNRAS*, 380, 1098
- Hansen, B. M. S., & Phinney, E. S. 1997, *MNRAS*, 291, 569
- Heggie, D. C. 1975, *MNRAS*, 173, 729
- Hils, D., Bender, P. L., & Webbink, R. F. 1990, *ApJ*, 360, 75
- Hopman, C., & Alexander, T. 2006, *ApJ*, 645, L133
- Hulse, R. A., & Taylor, J. H. 1975, *ApJ*, 195, L51

- Hurley, J. R., Pols, O. R., & Tout, C. A. 2000, *MNRAS*, 315, 543
- Hurley, J. R., Tout, C. A., & Pols, O. R. 2002, *MNRAS*, 329, 897
- Iben, Jr., I., & Tutukov, A. V. 1984, *ApJS*, 54, 335
- Iwasawa, M., An, S., Matsubayashi, T., Funato, Y., & Makino, J. 2011, *ApJ*, 731, L9
- Jiang, D., Han, Z., Ge, H., Yang, L., & Li, L. 2012, *MNRAS*, 421, 2769
- Kaspi, V. M., Bailes, M., Manchester, R. N., Stappers, B. W., & Bell, J. F. 1996, *Nature*, 381, 584
- Kroupa, P., Tout, C. A., & Gilmore, G. 1993, *MNRAS*, 262, 545
- Larson, S. L., Hiscock, W. A., & Hellings, R. W. 2000, *Phys. Rev. D*, 62, 062001
- Littenberg, T. B. 2011, *Phys. Rev. D*, 84, 063009
- Liu, J. 2009, *MNRAS*, 400, 1850
- Liu, J., Han, Z., Zhang, F., & Zhang, Y. 2010a, *ApJ*, 719, 1546
- Liu, J., Zhang, Y., Han, Z., & Zhang, F. 2010b, *Ap&SS*, 329, 297
- Liu, J., Zhang, Y., Zhang, H., Sun, Y., & Wang, N. 2012, *A&A*, 540, A67
- Lyne, A. G., & Lorimer, D. R. 1994, *Nature*, 369, 127
- Lyne, A. G., et al. 2004, *Science*, 303, 1153
- Mazeh, T., Goldberg, D., Duquennoy, A., & Mayor, M. 1992, *ApJ*, 401, 265
- Mestel, L. 1952, *MNRAS*, 112, 583
- Narayan, R., Paczynski, B., & Piran, T. 1992, *ApJ*, 395, L83
- Nelemans, G., Yungelson, L. R., & Portegies Zwart, S. F. 2001, *A&A*, 375, 890
- Nelemans, G. 2013, in *Astronomical Society of the Pacific Conference Series*, Vol. 467, 9th LISA Symposium, ed. G. Auger, P. Binétruy, & E. Plagnol, 27
- Nissanke, S., Vallisneri, M., Nelemans, G., & Prince, T. A. 2012, *ApJ*, 758, 131
- Nomoto, K., & Kondo, Y. 1991, *ApJ*, 367, L19
- Paczynski, B. 1976, in *IAU Symposium*, Vol. 73, Structure and Evolution of Close Binary Systems, ed. P. Eggleton, S. Mitton, & J. Whelan, 75
- Paczynski, B. 1991, *Acta Astron.*, 41, 257
- Petiteau, A., Auger, G., Haloïn, H., Jeannin, O., Plagnol, E., Pireaux, S., Regimbau, T., & Vinet, J.-Y. 2008, *Phys. Rev. D*, 77, 023002
- Podsiadlowski, P., Rappaport, S., & Han, Z. 2003, *MNRAS*, 341, 385
- Pols, O. R., Tout, C. A., Eggleton, P. P., & Han, Z. 1995, *MNRAS*, 274, 964
- Press, W. H., & Thorne, K. S. 1972, *ARA&A*, 10, 335
- Ruiter, A. J., Belczynski, K., Benacquista, M., Larson, S. L., & Williams, G. 2010, *ApJ*, 717, 1006
- Saio, H., & Nomoto, K. 1998, *ApJ*, 500, 388
- Schutz, B. F. 1996, *Classical and Quantum Gravity*, 13, 219
- Shah, S., van der Sluys, M., & Nelemans, G. 2012, *A&A*, 544, A153
- Shah, S., Nelemans, G., & van der Sluys, M. 2013, *A&A*, 553, A82
- Taam, R. E., & Sandquist, E. L. 2000, *ARA&A*, 38, 113
- Taylor, J. H., & Weisberg, J. M. 1982, *ApJ*, 253, 908
- Timpano, S. E., Rubbo, L. J., & Cornish, N. J. 2006, *Phys. Rev. D*, 73, 122001
- Tout, C. A., Aarseth, S. J., Pols, O. R., & Eggleton, P. P. 1997, *MNRAS*, 291, 732
- Tutukov, A. V., & Yungelson, L. R. 1994, *MNRAS*, 268, 871
- van der Sluys, M. V., Verbunt, F., & Pols, O. R. 2005, *A&A*, 431, 647

Wagoner, R. V., & Will, C. M. 1976, ApJ, 210,
764

Wang, B., Meng, X., Chen, X., & Han, Z. 2009,
MNRAS, 395, 847

Yungelson, L. R., Tutukov, A. V., & Livio, M.
1993, ApJ, 418, 794

Zhang, Y., Han, Z., Liu, J., Zhang, F., & Kang,
X. 2012, MNRAS, 421, 1678

Ziolkowski, J. 2010, Mem. Soc. Astron. Italiana,
81, 294